
Characterization of the SPECT 5-HT_{2A} Receptor Ligand ¹²³I-R91150 in Healthy Volunteers: Part 1—Pseudoequilibrium Interval and Quantification Methods

Ana M. Catafau^{1,2}, Monica Danus², Santiago Bullich², Jordi Llop³, Javier Perich⁴, Vincent J. Cunningham⁵, Pedro Plaza², Maria M. Penengo², Jos L.H. Eersels⁶, Lisa Squassante⁷, Domenec Ros⁸, and Manel Barbanjo⁹

¹Experimental Medical Sciences, Clinical Pharmacology Discovery Medicine, Psychiatry Centre of Excellence for Drug Discovery, GlaxoSmithKline, Barcelona, Spain; ²Centre for Imaging in Psychiatry, CRC-Mar, Hospital del Mar, Barcelona, Spain; ³Radiochemistry Laboratory, Institut d'Alta Tecnologia, PRBB-Fundació Privada, Barcelona, Spain; ⁴Magnetic Resonance Department, CRC-MAR, Hospital del Mar, Barcelona, Spain; ⁵Translational Medicine and Genetics, GlaxoSmithKline, Cambridge, United Kingdom; ⁶Department of Nuclear Medicine and PET Research, VU University Medical Center, Amsterdam, The Netherlands; ⁷Clinical Pharmacology Statistics and Programming, Biomedical Data Sciences, GlaxoSmithKline, Verona, Italy; ⁸Biophysics and Bioengineering Unit, University of Barcelona, Barcelona, Spain; and ⁹Clinical Pharmacology Unit, Hospital Sant Pau, Barcelona, Spain

With the aim of characterizing radioiodinated 4-amino-*N*-1-[3-(4-fluorophenoxy)propyl]-4-methyl-4-piperidinyl]5-iodo-2-methoxybenzamide (¹²³I-R91150) as a SPECT ligand for subtype 2A of the 5-hydroxytryptamine receptor (5-HT_{2A}), tracer kinetic compartmental analyses were compared with the tissue ratio method (TR). The pseudoequilibrium interval after a single bolus injection was identified, and a reference database of specific uptake ratio (SUR) values was obtained. Within-scan and between-subject variability was also assessed. **Methods:** Nineteen healthy men (mean age ± SD, 24.4 ± 3.3 y) were included and separated into 2 groups. Dynamic scans with venous blood sampling from 0 to 470 min after a single bolus injection of ¹²³I-R91150 was completed for 7 of the 9 subjects included in group A, and in one of them compartmental modeling was performed with an arterial blood input function using 1-tissue-compartment (1TC) and 2-tissue-compartment (2TC) models. Binding potential (BP) using the simplified reference tissue model (SRTM) (BP_{SRTM}) and SUR values using TR over time were also calculated. The 10 remaining subjects (group B) underwent a single scan at pseudoequilibrium with the aim of improving the precision of mean normal SUR estimates. Regions of interest in cortical regions and basal ganglia for specific uptake, and in cerebellum for nonspecific uptake, were manually drawn on each subject's MR images and translated to the corresponding SPECT slices after coregistration. **Results:** The 1TC model correlated well with the 2TC model (BP_{2TC} = 1.04·BP_{1TC} - 0.01, R² = 0.98), and both methods correlated with BP_{SRTM} and SUR with little bias (BP_{1TC} = 1.10 BP_{SRTM} + 0.03, R² = 0.98; BP_{2TC} = 1.15 BP_{SRTM} + 0.01, R² = 0.98; BP_{SRTM} = 0.99 SUR_{mean} + 0.01, R² = 0.98). SUR values stabilized from 180 min after injection in most cortical regions, ranging from 0.51 ± 0.10 in the orbitofrontal region to

0.27 ± 0.09 in the parietal region. Within-scan and between-subject variability among regions ranged from 10% to 14.8%, and from 18.3% to 35.4%, respectively. **Conclusion:** ¹²³I-R91150 distribution agrees with autoradiography results, showing highly specific binding in cortical regions. The correlations found among 1TC, 2TC, SRTM, and TR outcome measurements support the use of TR for quantification of 5-HT_{2A} receptor binding with ¹²³I-R91150 SPECT and a simple protocol avoiding arterial blood sampling and serial scanning over time.

Key Words: molecular imaging; neurotransmission; SPECT; ¹²³I-R91150; 5-HT_{2A}

J Nucl Med 2006; 47:919–928

Radioiodinated 4-amino-*N*-1-[3-(4-fluorophenoxy)propyl]-4-methyl-4-piperidinyl]5-iodo-2-methoxybenzamide (¹²³I-R91150) is a suitable ligand for SPECT imaging of subtype 2A of the 5-hydroxytryptamine receptor (5-HT_{2A}) in the human brain. ¹²³I-R91150 SPECT has been used to investigate several psychiatric disorders (1–6) and to measure drug-induced 5-HT_{2A} receptor occupancy (7–10). In these previous studies, a single SPECT acquisition after bolus injection was used to calculate the specific uptake ratio (SUR) using the simple tissue ratio method (TR) at pseudoequilibrium. Because of its simplicity, this method optimizes scanning feasibility and the subject's compliance. However, validation of TR against kinetic compartmental analysis in humans is still needed.

The present study aimed to characterize ¹²³I-R91150 as a SPECT radioligand for assessment of cerebral 5-HT_{2A} receptors in healthy volunteers. Tracer kinetic compartmental analyses based on dynamic time-course data with an arterial plasma input function and the simplified reference

Received Dec. 23, 2005; revision accepted Mar. 1, 2006.
For correspondence or reprints contact: Ana M. Catafau, MD, Centre for Imaging in Psychiatry, GlaxoSmithKline, Psychiatry CEDD, Torre Mapfre, Villa Olímpica, La Marina, 16-18, Pl. 9 B y C, 08005-Barcelona, Spain.
E-mail: ana.m.catafau@gsk.com

tissue model (SRTM) were compared using TR. The pseudoequilibrium interval after a single bolus injection was identified, and a reference database of SUR values was obtained. Moreover, within-scan variability at pseudoequilibrium, between-subject variability, and ^{123}I -R91150 behavior in plasma were assessed. The specificity of ligand binding to the 5-HT_{2A} receptor and confirmation of the cerebellum as a reference region for SUR calculations was investigated by means of a ketanserin displacement study reported separately (11).

MATERIALS AND METHODS

Subjects

Nineteen men (mean age \pm SD, 24.4 ± 3.3 y) determined through the Structured Clinical Interview for DSM-IV to be healthy were enrolled in this study. None had a history of psychiatric treatment or significant medical events. None was taking psychotropic drugs or other relevant medication. Absence of illegal drug abuse was assessed by questioning and supported by urine drug screening (InstaCheck Drug Screen Test; Applied Biotech/Forefront Diagnostics). Subjects had to withdraw from caffeine and alcohol 24 h before the study day and were not allowed to take any drugs during the 7 d before the study day. All had normal findings on physical examination, 12-lead electrocardiography, clinical chemistry, and hematology. The study was approved by the local Ethics Committees and the Spanish Ministry of Health, and written informed consent was obtained from all subjects before inclusion in the study.

Synthesis of ^{123}I -R91150

Radioiodination by direct electrophilic substitution was performed on the 5-position of the methoxybenzamide group of 4-amino-*N*-[1-[3-(4-fluorophenoxy)propyl]-4-methyl-4-piperidinyl]-2-methoxybenzamide by means of *in situ*-prepared peracetic acid and no-carrier-added Na ^{123}I (Tyco Healthcare) to obtain ^{123}I -R91150, as reported previously (12). Briefly, 500 μL of no-carrier-added Na ^{123}I (+ carrier; 0.532 nmol of sodium iodide per 37 MBq of ^{123}I) were added to a V-vial containing 40 μg of R91150 in 300 μL of glacial acetic acid. To this solution, 100 μL of H₂O₂ (30% solution) were added in 4 steps at 0, 10, 20, and 25 min. The reaction was stopped at 30 min with 0.5 mL of a 0.5 mol/L solution of sodium sulfite in a 4.5 mol/L solution of NaOH. After labeling, the reaction mixture (volume, 1–2 mL) was injected into a guard column (C-1035, 10 \times 10 mm; Upchurch England) filled with Perisorb RP-8 resin [Merck] and further purified by means of high-performance liquid chromatography (HPLC) (RP Select B, [Merck] 250 \times 4 mm, 10 μm with an isotonic ethanol/acetate solution as eluent). The collected ^{123}I -R91150 fraction was further diluted with an isotonic citrate/acetate buffer (end pH, 6.0–6.4), filtered through a Millex-FG filter (Millipore), and autoclaved. The filter was pretreated with ethanol and rinsed with diluent to avoid stickiness. A trace of *o*-iodo-hippuric acid (1 mg/mL of diluent) was added to the diluent to prevent deiodination during autoclaving and transportation. The specific activity of the autoclaved ^{123}I -R91150 was approximately 300 TBq/mmol. Radiochemical purity at the time of administration (i.e., 24 h after synthesis) was higher than 96%.

Subject Preparation and SPECT Procedure

SPECT was performed using a 3-head Prism 3000S camera (Philips) fitted with ultra-high-resolution fanbeam collimators. The preparation of each subject included administration of potassium perchlorate (8 mg/kg) up to 20 min before ^{123}I -R91150 injection to minimize exposure of the thyroid gland to radiation. Four multimodality SPECT/MRI markers (MM3003; IZI Medical Products Corp.), each filled with approximately 0.074 MBq of ^{123}I , were firmly attached to the subject's head at the level of the mastoids and the corners of the eyes and remained in the same position until both the SPECT and the MRI acquisitions were finalized.

The subjects were separated into 2 groups. Group A consisted of 9 healthy men (mean age, 24.4 ± 3.2 y; range, 20–29 y) who underwent sequential SPECT over time with blood sampling. Scanning sessions consisted of one 10-min, five 30-min, and three 40-min frames collected using a 360° circular orbit, step-and-shoot mode every 30°, on a matrix size of 128 \times 128 pixels, starting at 0, 11, 71, 120, 180, 240, 330, 400, and 470 min after injection. The subjects were allowed to rest outside the SPECT camera during breaks between acquisitions. A venous catheter for blood sampling was inserted in the arm opposite the radioligand injection in all subjects. An additional catheter for arterial blood sampling (Leader Cath Arteriel 18 G; Laboratoires Pharmaceutiques) was placed in the radial artery after local anesthesia with lidocaine 2% in 1 subject. ^{123}I -R91150 (148–222 MBq) was injected intravenously when the acquisition began and was flushed with 20 mL of saline serum. Two of the 9 subjects in group A could not complete the entire scan session because of a camera breakdown, but venous blood samples were drawn for radioligand analysis up to 470 min after injection. Therefore, in a total of 7 subjects (mean age, 23.4 ± 2.6 y; range, 20–27 y), the entire scanning session was completed.

Group B consisted of 10 healthy men (mean age, 24.3 ± 3.6 y; range, 20–29 y) who underwent a 30-min scan starting at 180 min after injection.

MRI

All subjects underwent T1-weighted 3-dimensional MRI on the same day as the SPECT scan using a superconductive 1.9-T system (Prestige 2T; GE Healthcare) equipped with a head coil. An axial 3-dimensional spoiled gradient-echo slab was positioned to include the entire head, and images were acquired with the following parameters: repetition time, 25 ms; echo time, 6 ms; flip angle, 28°; field of view, 25 \times 25 cm; matrix, 256 \times 256; section thickness, 2 mm with no interslice gap; and number of excitations, 1.

Image Processing

Images were reconstructed using a filtered-backprojection algorithm with a Butterworth filter (exponent, 5.0; cutoff frequency, 0.4 cycle/pixel). Pixel sizes were between 2.44 and 2.52 mm on each slice and 3.6 mm in the axial direction. Attenuation correction was performed using the Chang algorithm and a manually fitted elliptic attenuation map on each slice ($\mu = 0.1 \text{ cm}^{-1}$). SPECT and MRI scans were registered using in-house software implemented in C language. First, the corresponding external markers were manually identified on the MRI and SPECT scans. Then, rigid-body transformation (3 translations and 3 rotations) was estimated automatically by minimizing the sum of the squared distances between the corresponding marker positions (13).

Regions of interest (ROIs) were drawn manually by the same investigator on the MR image of the frontal, temporal, occipital,

and parietal lobes and the thalamus, striatum, and cerebellum. The frontal lobe was divided into orbitofrontal, prefrontal, and superior frontal regions. The temporal lobe was divided into mesial (including amygdala and hippocampus) and lateral (temporal cortex) regions, and the occipital lobe was divided into calcarine and lateral regions.

Data Analysis

Tracer kinetic modeling including 1TC and 2TC analysis and SRTM were used for data analysis, and the results were compared with those obtained with TR.

The 1TC and 2TC analyses were applied to the subject who provided arterial blood samples. The 2TC model assumes that the activity in tissue can be separated into 2 compartments: Free and nonspecifically bound compartments are considered a single compartment, and specifically bound tracer is considered another compartment. The 1TC model assumes that the free, nonspecifically bound, and specifically bound compartments all equilibrate rapidly and may be considered a single compartment. The set of regional time–activity curves was fitted to the 1TC and 2TC models using the metabolite-corrected plasma input curves, and the total volume of distribution (VD) was calculated for both models (the blood volume component was fixed to 5%). Equations used to calculate VD are described in Erlandsson et al. (14). Binding potential (BP) in 1TC (BP_{1TC}) and 2TC (BP_{2TC}) models was calculated as $(VD_{Sp} - VD_{Ref})/VD_{Ref}$, where VD_{Sp} and VD_{Ref} were the VDs in the region with specific uptake and in the reference region (cerebellum). The VD_{Ref} was always calculated using 1TC.

Quantification using the SRTM was applied to all subjects from group A who underwent the entire SPECT session ($n = 7$). Cerebellum time–activity curves were used to provide the input function to the kinetic model. BP using SRTM (BP_{SRTM}) was the outcome measurement, as described in Lammertsma et al. (15). TR was applied to all subjects (groups A and B, $n = 17$). SUR values were calculated as $[(C_{reg} - C_{cer})/C_{cer}]$, where C_{reg} and C_{cer} were the mean counts at pseudoequilibrium in the studied cerebral region and in the cerebellum, respectively. SUR curves over time were obtained from group A, and the pseudoequilibrium interval was defined as the period during which SUR values were stable.

Plasma Analysis

Plasma analysis of ^{123}I -R91150 was performed for 9 subjects. A total of 16 venous blood samples were collected manually, at -1 (baseline), 0.25, 0.5, 1, 1.5, 2, 5, 10, 15, 71, 120, 180, 240, 330, 400, and 470 min after injection, in all subjects. In 1 subject, venous and arterial blood samples were collected simultaneously. Arterial and venous blood samples were processed by the same procedure. The first blood sample (at -1 min), which contained no activity, was extracted as a reference. Samples 2–16 were separated into 2 fractions (1 mL each), introduced into 1.5-mL flasks with a micropipette, and centrifuged at 2,000g for 4 min. The plasma fraction was separated, and both the plasma and the residue fractions were counted in a γ -counter (2200 Scaler Ratemeter; Ludlum Measurements Inc.) for 30 s. All samples were further processed by analytic HPLC to determine the fraction of plasma activity representing unmetabolized radiotracer. For this purpose, 1 mL of pure acetonitrile was added to the plasma fraction, and after being mixed for 20 s, the samples were centrifuged at 2,000g for 4 min. The liquid phase was separated from the precipitate by decantation, and both fractions were

counted in the γ -counter. For HPLC analysis, both liquid phase fractions corresponding to the same blood sample were joined, and the resulting solution was evaporated at 40°C under a continuous flow of helium. The residue was diluted in 100 μL of mobile phase and injected into the HPLC system. The HPLC system consisted of an 1100 series chromatograph (Agilent Technologies) equipped with a 1100 series isocratic pump, a Rheodyne injector with a 20- μL loop, a temperature-controlled column compartment (temperature set-point, 25°C), and a ZORBAX Eclipse XDB-C8 column (4.6 \times 150 mm, 15 μm ; Agilent Technologies) and a γ -detection system (GABI; Raytest) equipped with a 250- μL flow cell. The whole system was controlled by Gina-Star software (Raytest), with decay correction in real time. The detection energy window was adjusted to 159 ± 50 keV. A 65:35 mixture of acetonitrile:water was used as the mobile phase. The chromatographic runs were performed under isocratic conditions, at a flow of 1 mL/min, with a total chromatographic time of 12 min.

From the first blood sample (extracted before radiotracer injection), two 1-mL samples were separated and introduced into 1.5-mL flasks, and 100 μL of ^{123}I -R91150 reference solution (~ 370 kBq/mL, measured with a dose calibrator [Pet Dose; Comecer]) were added to each. The resulting solutions were submitted to the same experimental procedure as described for samples 2–16 (or, eventually, 2–17). Sample 1 was used to determine the retention time of the parent compound under chromatographic conditions and to calculate the relationship between activity concentration in plasma and obtained counts in the γ -counter. All samples were processed within 60 min after blood sampling.

Statistical Analysis

The SAS, version 8.02, system (SAS Institute Inc.) and procedures for Windows (Microsoft) were used for all statistical analyses. In group A, the pseudoequilibrium interval was assessed on the time profile of SUR values. Over the time during which the SUR curves were expected to be at steady state on the basis of visual inspection of the SUR–time curves, a mixed-model regression analysis was fit for each region separately, with time as a continuous covariate and subject as a random effect. The slopes and corresponding 95% confidence intervals were estimated for each brain region. Within-scan variability at pseudoequilibrium was estimated by the regression model and was provided along with between-subject variability over the time at pseudoequilibrium. The relationship between BP (using 1TC, 2TC, and SRTM) and SUR was analyzed by means of Pearson correlations.

RESULTS

^{123}I -R91150 Cerebral Distribution and Brain Kinetics

^{123}I -R91150 showed the highest accumulation in cerebral cortex, with low uptake in striatum and thalamus and negligible uptake in cerebellum (Fig. 1). Given the low uptake in basal ganglia, only cortical regions were considered for the graphical representation of results. Mean decay-corrected regional time–activity curves (Fig. 2) showed the cerebellum as the region with the earliest peak (10–40 min after injection) and lowest activity. Cortical regions showed specific binding and peaked later, between 120 and 180 min after injection.

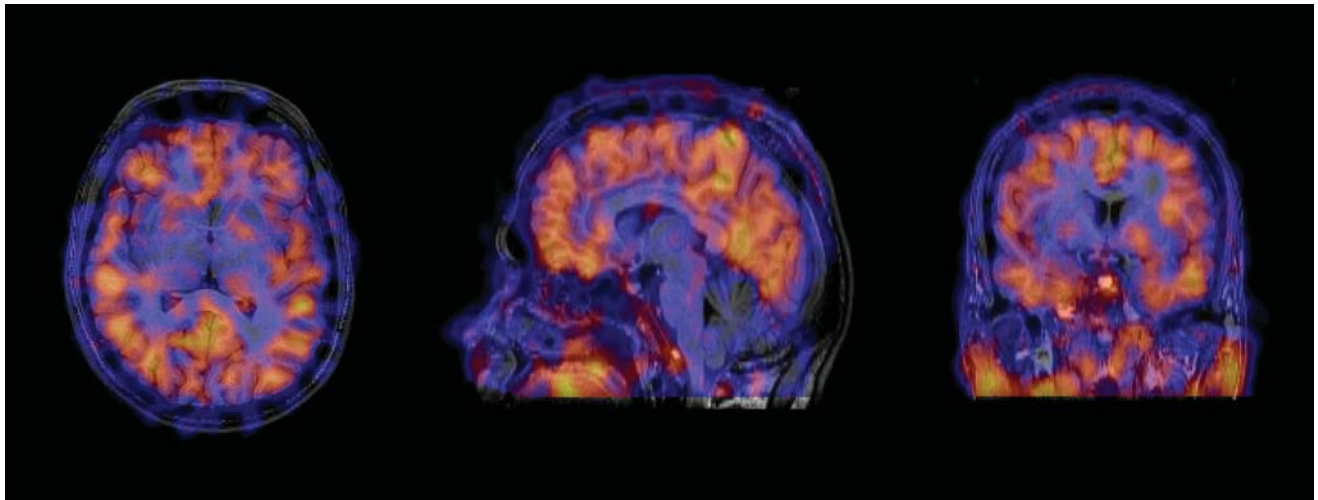


FIGURE 1. Transverse (left), sagittal (center), and coronal (right) views of coregistered MRI/SPECT images showing cerebral distribution of ^{123}I -R91150 in healthy volunteer. Added SPECT images were obtained from 180 to 270 min after injection. Uptake is predominant in cortex and negligible in cerebellum.

Tracer Kinetic Modeling

Full kinetic modeling with arterial sampling yielded similar BP values using either 1TC or 2TC, which correlated strongly ($\text{BP}_{2\text{TC}} = 1.04 \text{BP}_{1\text{TC}} - 0.01$, $R^2 = 0.98$) (Fig. 3A). BP_{SRTM} correlated with $\text{BP}_{1\text{TC}}$ and $\text{BP}_{2\text{TC}}$ with a small bias ($\text{BP}_{1\text{TC}} = 1.10 \text{BP}_{\text{SRTM}} + 0.03$, $R^2 = 0.98$; $\text{BP}_{2\text{TC}} = 1.15 \text{BP}_{\text{SRTM}} + 0.01$, $R^2 = 0.98$) (Fig. 3B). With all methods, the highest BP from the cortical regions corresponded to the orbitofrontal region ($\text{BP}_{1\text{TC}} = 0.79$, $\text{BP}_{2\text{TC}} = 0.80$, $\text{BP}_{\text{SRTM}} = 0.67$) and the lowest to the parietal region ($\text{BP}_{1\text{TC}} = 0.44$, $\text{BP}_{2\text{TC}} = 0.45$, $\text{BP}_{\text{SRTM}} = 0.38$).

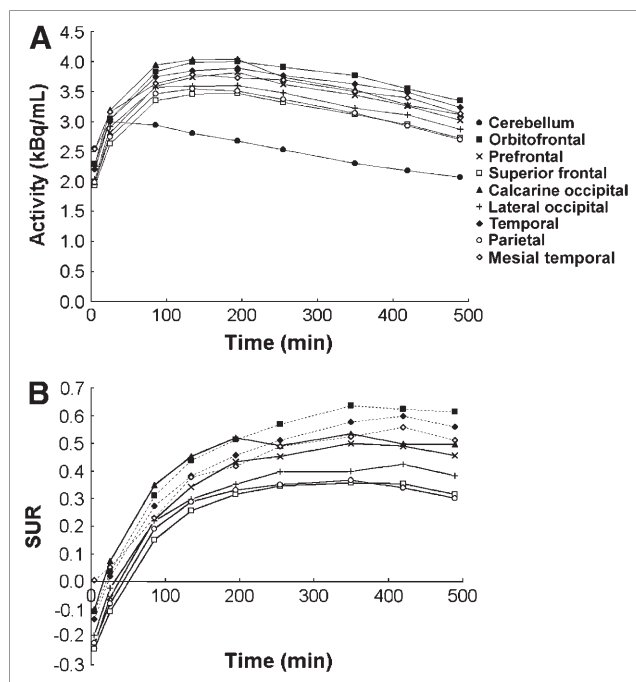


FIGURE 2. (A) Decay-corrected mean time-activity curves in cerebellum and cortical regions. (B) SUR values over time for all cortical regions studied.

TR and Pseudoequilibrium Interval

Plots of mean SUR values over time (group A) for all regions studied are shown in Figure 2. In all regions, uptake progressively increased until 180–240 min after injection and then stabilized until the end of the scanning session. The pseudoequilibrium interval was determined by analyzing the slopes of SUR values over time during the visually identified steady state, that is, from 180 to 470 min after injection and from 240 to 470 min after injection. Slopes and corresponding 95% confidence intervals are reported in Table 1. The 95% confidence interval of the slope of the fitted regression line lacked significance from 180 min after injection until the end of the study in all regions except the orbitofrontal and temporal (lateral and mesial) cortices, which reached steady state at 240 min after injection. In these regions, the SUR values were consistently lower at 180 min after injection (SUR_{180}) than at their pseudoequilibrium time (SUR_{240}). The average differences between SUR_{180} and SUR_{240} were $9.5\% \pm 8.1\%$ for the orbitofrontal region, $14.8\% \pm 16.4\%$ for the temporal, and $21.1\% \pm 12.4\%$ for the mesial temporal.

SRTM Versus TR

BP_{SRTM} , mean SUR_{180} , within-scan variability, and between-subject variability are shown in Table 2. Striatum and thalamus showed faint uptake. In the cortex, the highest BP and SUR values corresponded to the orbitofrontal and temporal (lateral and mesial) regions, followed by the calcarine occipital and prefrontal regions. Moderate specific binding was found in the remaining cortical regions (lateral occipital, superior frontal), and the lowest corresponded to the parietal lobe.

Scatter plots comparing BP_{SRTM} and SUR are shown in Figure 4. The best correlation was found when the mean SUR values of the whole pseudoequilibrium interval for each region (SUR_{mean}) were considered—that is, 240–470

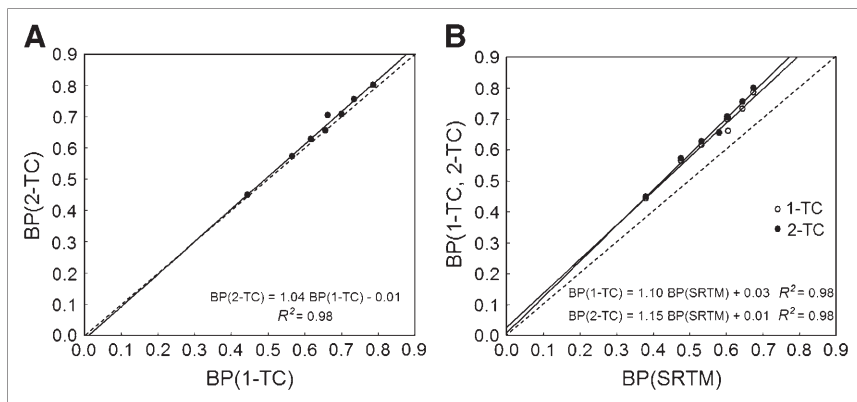


FIGURE 3. (A) Scatter plot of BP_{1TC} vs. BP_{2TC} . (B) Scatter plot of BP_{SRTM} vs. BP_{1TC} and BP_{2TC} .

min after injection for the orbitofrontal and temporal regions and 180–470 min after injection for all the remaining regions ($BP_{SRTM} = 0.99 SUR_{mean} + 0.01$, $r = 0.98$) (Fig. 4A). Good correlations were also found when a single SUR value at pseudoequilibrium for each region was used—that is, SUR_{240} for the orbitofrontal and temporal regions and SUR_{180} for all remaining regions ($BP_{SRTM} = 0.85 SUR_{180/240} + 0.09$, $r = 0.88$) (Fig. 4B). Finally, SUR_{180} was considered for all regions ($BP_{SRTM} = 0.89 SUR_{180} + 0.09$, $r = 0.79$). In that case, the orbitofrontal and temporal regions showed the most underestimated SUR values with respect to the BP_{SRTM} values (Fig. 4C).

The within-scan variability of the SUR values obtained throughout the entire pseudoequilibrium interval (180–470 min after injection, group A) ranged from 10% to 14.8% across all cortical regions (Table 2). The prefrontal and

lateral temporal cortices showed the lowest within-scan variability, and the superior frontal and parietal showed the highest. Between-subject variability over the pseudoequilibrium period ranged from 18.3% to 35.4% in the cortex. The temporal cortex (both lateral and mesial) was the least variable area (18.3%–18.9%), and the superior frontal was the most variable (35%) (Table 2). The basal ganglia showed high variability, both within scans (>33%) and between subjects (>40%).

Plasma Analysis

Average total activity and unmetabolized parent-compound activity in plasma curves obtained from venous samples of the 9 subjects plateaued after a rapid distribution phase (Figs. 5A and 5B). Figures 5C and 5D show the fraction of the activity corresponding to unmetabolized parent compound in plasma (arterial and venous blood) as a function of time for the subject who provided arterial blood samples. Activity peaks were found at 0.8 and 2 min for arterial and venous curves, respectively. The maximum activity reached in the venous blood curve was around 12 times lower than that reached in the arterial blood curve. Both curves were almost identical 10 min after injection.

The percentage of unmetabolized parent compound over time is presented in Figure 6A (average values for venous blood samples, $n = 9$). Ten minutes after injection, the fraction of activity corresponding to unmetabolized parent compound in plasma dropped from the initial value of $97\% \pm 2\%$ to $88\% \pm 3\%$. Afterward, a slow decrease was observed until its final level ($76\% \pm 8\%$) was reached. The chromatograms obtained for samples drawn from 1 subject at -1 , 2, and 240 min after injection of the radiotracer are depicted in Figure 6B. Only 1 species more hydrophilic than the parent compound (lower retention time) could be detected in all chromatograms. Comparison of the chromatograms evidenced that the relative size of the peak with a retention time of approximately 1.5 min increased with time, whereas the peak with a retention time of approximately 6 min (corresponding to unmetabolized parent compound) decreased with time, reaching a relative size of $76\% \pm 8\%$ of total activity in the plasma fraction at 470 min after injection. Although there is no experimental

TABLE 1

Linear Regression Analysis Slopes and 95% Confidence Intervals for Group A ($n = 7$) at 180–470 and 240–470 Minutes After Injection

| Cortical region | Slope, SUR/h | |
|------------------|--------------------|---------------------|
| | 180–470 min | 240–470 min |
| Frontal | | |
| Orbitofrontal | 0.03 (0.01, 0.04) | 0.02 (−0.01, 0.04) |
| Prefrontal | 0.01 (0.00, 0.02) | 0.00 (−0.01, 0.02) |
| Superior frontal | 0.01 (0.00, 0.02) | 0.01 (−0.02, 0.04) |
| Temporal | | |
| Lateral | 0.02 (0.01, 0.04) | 0.01 (0.00, 0.03) |
| Mesial | 0.02 (0.01, 0.04) | 0.01 (−0.01, 0.03) |
| Occipital | | |
| Calcarine | 0.00 (−0.02, 0.01) | 0.00 (−0.02, 0.02) |
| Lateral | 0.01 (0.00, 0.02) | 0.00 (−0.01, 0.02) |
| Parietal | 0.00 (−0.01, 0.01) | −0.01 (−0.03, 0.00) |
| Striatum | 0.02 (0.00, 0.03) | 0.00 (−0.02, 0.02) |
| Thalamus | 0.01 (−0.01, 0.03) | 0.02 (0.00, 0.04) |

Data in parentheses are 95% confidence intervals. Intervals including 0 indicate slope not significantly different from 0 and therefore pseudoequilibrium interval. Intervals not including 0 indicate radioligand not at equilibrium.

TABLE 2

Mean (\pm SD) SUR₁₈₀ and BP_{SRTM}, Between-Subject Variability, and Within-Scan Variability for Group A ($n = 7$)

| Region | SUR ₁₈₀ group A | Between-subject variability (%) | Within-scan variability (%) | BP _{SRTM} (mean \pm SD) |
|------------------|-----------------------------------|---------------------------------|-----------------------------|------------------------------------|
| Frontal | | | | |
| Orbitofrontal | 0.50 \pm 0.09 (0.46 \pm 0.11) | 19.6 | 11.3 | 0.61 \pm 0.11 |
| Prefrontal | 0.43 \pm 0.10 (0.38 \pm 0.13) | 20.6 | 10.0 | 0.46 \pm 0.09 |
| Superior frontal | 0.30 \pm 0.12 (0.30 \pm 0.10) | 35.4 | 14.8 | 0.32 \pm 0.11 |
| Temporal | | | | |
| Lateral | 0.46 \pm 0.07 (0.43 \pm 0.10) | 18.9 | 10.5 | 0.56 \pm 0.09 |
| Mesial | 0.40 \pm 0.06 (NA) | 18.3 | 13.9 | 0.53 \pm 0.09 |
| Occipital | | | | |
| Calcarine | 0.51 \pm 0.10 (0.45 \pm 0.12) | 19.1 | 14.6 | 0.49 \pm 0.07 |
| Lateral | 0.34 \pm 0.08 (0.34 \pm 0.11) | 24.8 | 13.3 | 0.38 \pm 0.10 |
| Parietal | 0.31 \pm 0.07 (0.27 \pm 0.09) | 22.4 | 14.7 | 0.32 \pm 0.06 |
| Striatum | 0.11 \pm 0.06 (NA) | 54.2 | 36.7 | 0.24 \pm 0.15 |
| Thalamus | 0.23 \pm 0.08 (NA) | 41.6 | 33.0 | 0.22 \pm 0.12 |

NA = not available.

Data in parentheses are SUR₁₈₀ values for groups A and B ($n = 17$).

evidence of the structure of the radioactive species, co-injection with free ¹²³I-iodine showed the same retention time as for the first peak (\sim 1.5).

The fraction of activity in plasma over time (referred to as total blood activity) is shown in Figure 7 (average values for venous blood samples, $n = 9$). The fraction of activity in plasma decreased quickly (<15 min), reaching a plateau of around 80% at 15 min after injection.

DISCUSSION

¹²³I-R91150 Cerebral Distribution and Brain Kinetics

Serotonin receptors are broadly distributed in the brain. Using human brain autoradiography, the highest densities of 5-HT₂ receptors have been reported in the cerebral cortex and the lowest in the thalamus, striatum, and cerebellum (16). These findings agree with the predominantly cortical distribution and corresponding ¹²³I-R91150 BP and SUR values shown in the present study.

The brain kinetics of ¹²³I-R91150 were previously described in 2 subjects (17). In that study, the cerebellum was found to peak at 5 min after injection and the frontal cortex at 100–120 min after injection. The present study showed slightly slower kinetics. Although the acquisition times in the present study did not allow accurate identification of the time at peak for these regions, the cerebellum was shown to peak between 10 and 40 min after injection and cortical regions between 120 and 180 min after injection (Fig. 2). The larger sample size in the present study may account for such a difference in timing of the peaks.

Tracer Kinetic Modeling and TR

The TR method, because it does not require either blood sampling or long scanning sessions over time, is desirable but may lead to a biased estimation of BP. The present study compared tracer kinetic compartmental analyses based on dynamic time-course data and an arterial plasma

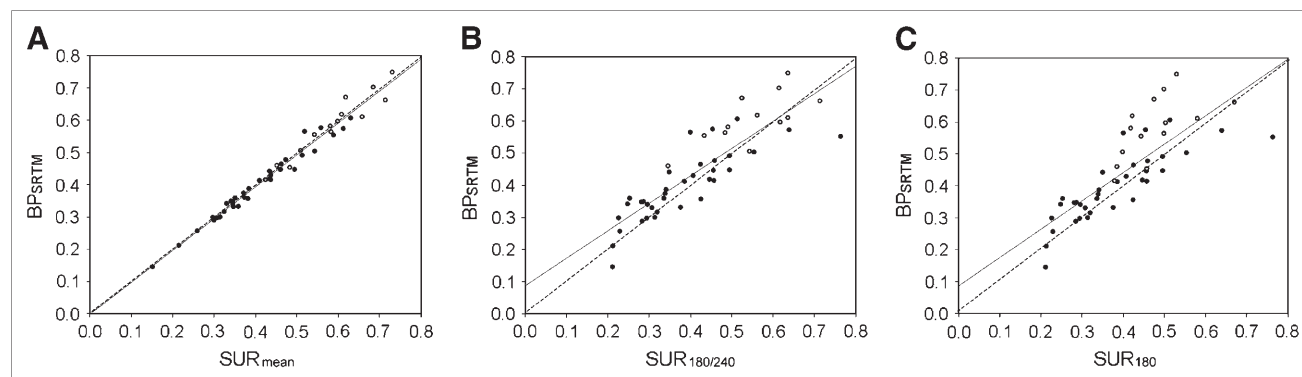


FIGURE 4. Scatter plots comparing BP_{SRTM} and SUR in orbitofrontal and temporal regions (○) and remaining cortical regions (●). (A) In this plot, mean SUR values of entire pseudo-equilibrium interval (SUR_{mean}) were considered (i.e., from 240 to 470 min after injection for orbitofrontal and temporal regions and from 180 to 470 min after injection for all remaining regions). (B) In this plot, single SUR value at pseudo-equilibrium for each region was considered (i.e., SUR₂₄₀ for orbitofrontal and temporal regions and SUR₁₈₀ for all remaining regions). (C) In this plot, SUR₁₈₀ was considered for all regions.

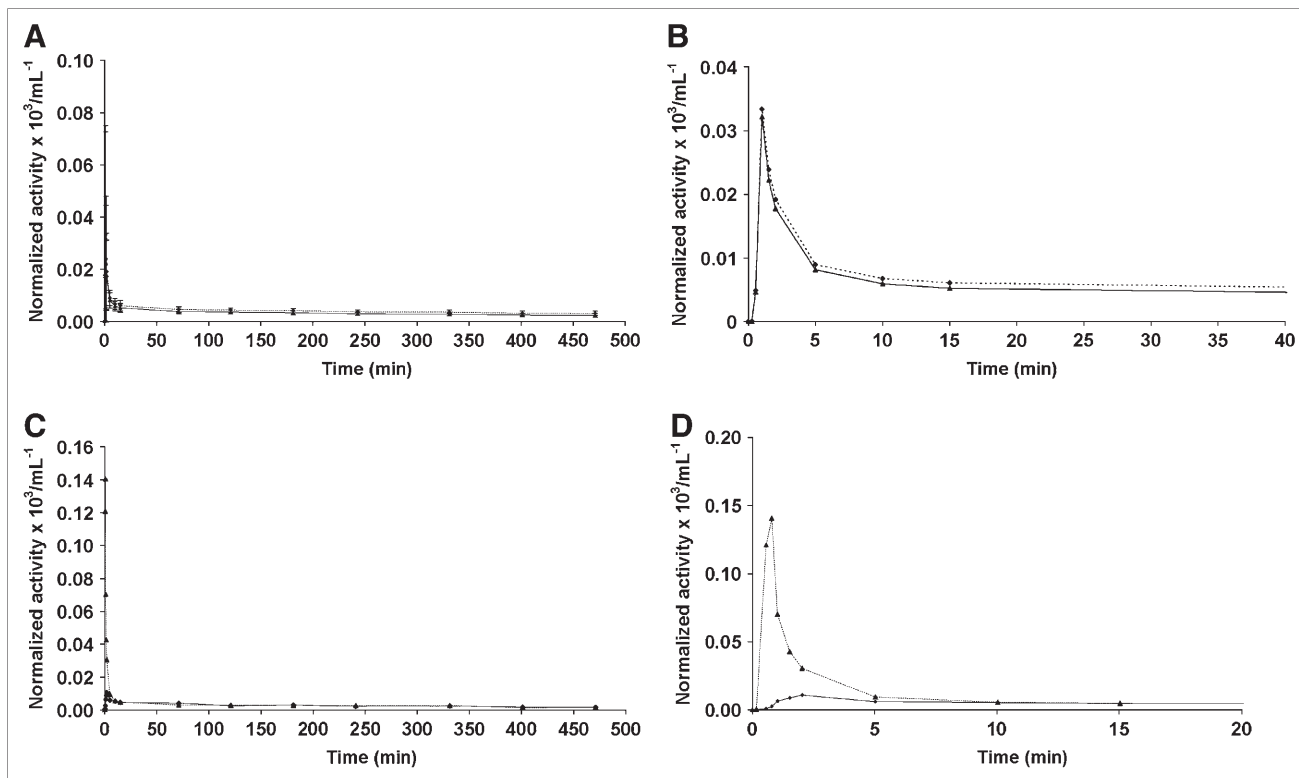


FIGURE 5. (A and B) Averages obtained from data of 9 subjects in group A. Total plasma activity (dotted line) and activity corresponding to unmetabolized parent compound (solid line) in plasma are shown as function of time for entire study (A) and for first 40 min after injection (B). (C and D) Data of subject who provided arterial blood samples. Activity corresponding to unmetabolized parent compound in plasma is shown as function of time for venous (solid line) and arterial (dotted line) blood samples for entire study (C) and for first 20 min after injection (D). All values are decay corrected to injection time and normalized with injected activity.

input function with TR to validate the specific binding measurements obtained using the simplest methodology.

An excellent correlation was found between BP_{1TC} and BP_{2TC} , thus validating and supporting the use of SRTM for quantification of ^{123}I -R91150 SPECT. BP_{SRTM} was shown to be approximately 10% lower than BP_{1TC} and approxi-

mately 15% lower than BP_{2TC} (Fig. 3). Furthermore, BP_{SRTM} values also correlated with SUR values. Although the best correlation was found when the whole pseudoequilibrium interval was used for SUR calculations, a good correlation was still found when a single SUR value at pseudoequilibrium was used (Fig. 4). This finding suggests that TR can

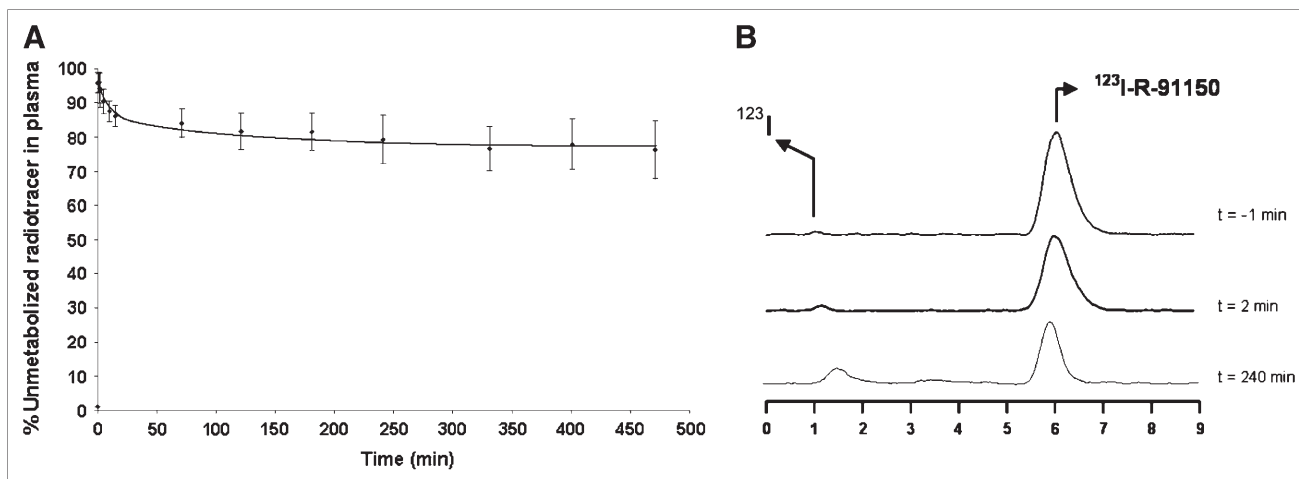


FIGURE 6. (A) Percentage of unmetabolized parent compound in plasma as function of time. (B) Chromatograms obtained for samples extracted at -1, 2, and 240 min after injection.

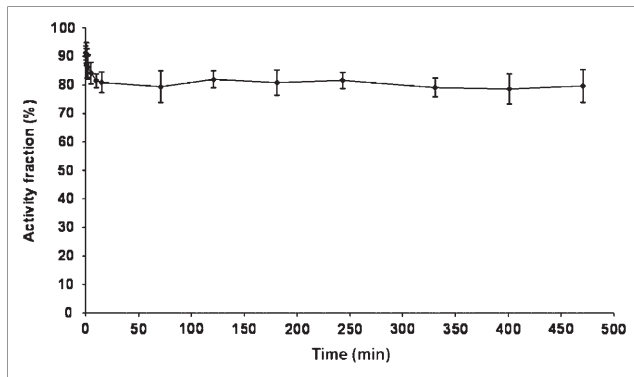


FIGURE 7. Fraction of activity in plasma vs. time, referred to as total blood activity.

be applied for quantification of 5-HT_{2A} receptor binding using ¹²³I-R91150 SPECT with a simple protocol avoiding arterial blood sampling and serial scanning over time.

In this study, the cerebellum was used as a reference region for both SRTM and SUR quantification. The cerebellum is virtually free of 5-HT₂ receptors (18) and has consistently been chosen as a reference region for SUR calculations (1–6,19,20). The appropriateness of the cerebellum as a reference region was previously supported by the lack of ¹²³I-R91150 displacement induced by ketanserin in the cerebellum in a preliminary study (21,22), as well as in our own experience (11). The excellent correlation found between BP values calculated with full kinetic modeling (1TC and 2TC) and SRTM in the present study also supports the suitability of the cerebellum as a reference region for ¹²³I-R91150 SPECT quantification.

Pseudoequilibrium Interval for TR

Despite the importance of accurate identification of the pseudoequilibrium interval for SUR calculations after a single radioligand injection, to the best of our knowledge ¹²³I-R91150 SUR values over time have been reported for a total of only 3 healthy volunteers from 2 different groups. Busatto et al. (17) scanned 2 healthy volunteers over time, one up to 880 min after injection and another up to 200 min after injection. These subjects showed stable frontal–cerebellar activity ratios from 100 min after injection. Audenaert et al. (2) reported the presence of a frontal–cerebellar ratio curve up to 168 min after injection in an additional healthy volunteer and proposed 110–140 min after injection as the appropriate scanning time. Besides the limitations arising from the small sample sizes, assessment of the pseudoequilibrium interval was limited by being performed visually from the time–activity curves in both cases. Therefore, further evaluation was needed. Data from the present study for 7 healthy volunteers scanned up to 470 min after injection showed that in most cortical regions, SUR values progressively increased until 180 min after injection and then remained stable through the end of the scanning session. This stability was confirmed by linear regression analysis showing that for most cortical regions, the slope

within this interval did not significantly differ from 0. We therefore suggest that 180 min after injection be selected as the earliest time for ¹²³I-R91150 SPECT acquisition after a single radioligand injection. Identification of the earliest time at which the radioligand reaches pseudoequilibrium is important because minimizing the length of the exploration improves patient compliance and economics in the clinical setting. When measurements in the orbitofrontal and temporal regions are of particular interest, an approximately 10%–20% underestimation in the SUR₁₈₀ should be considered. Although stable SUR values were maintained up to 470 min after injection in all regions, late frames are not recommended for quantification given the lower counting rate due to isotope decay.

Normal Database of SUR₁₈₀ and Variability of Measurements

The present study showed the highest SUR₁₈₀ to be in the orbitofrontal and temporal regions, followed by the remaining cortical regions from occipital calcarine to parietal in descending order (Table 2). The basal ganglia showed the lowest SUR₁₈₀ and the highest variability. A summary of previously reported mean cortical SUR values in healthy volunteers by other groups is presented in Table 3. Busatto et al. (17) and Travis et al. (7), both from the same group in London, reported values from 0.40 to 0.44 in different cortical regions when scanning at 250 min after injection (17) and lower values (0.30–0.38) when scanning at 120 min (7). Audenaert et al. (2,19), van Heeringen et al. (1), and Versjijt et al. (3), from the same group in Ghent, performed a 40-min scan starting between 110 and 140 min after injection and reported higher values overall, ranging from 0.52 to 1.03 depending on the cerebral region and the study (Table 3). Finally, Reneman et al. (5,20) and Baeken et al. (24), using different acquisition protocols but starting the acquisition at the same time (120 min) after injection, found intermediate SUR values, ranging from 0.74 (20) to 0.87 (24). Differences in methodology can account for the variation among reported SUR values. The time of scanning is an important factor. The SUR–time curves obtained in the present study showed that SUR values were underestimated when calculated before the pseudoequilibrium interval had been reached (Fig. 2). Other factors include scanner resolution and sensitivity, reconstruction parameters, and the ROI method used (e.g., MRI–SPECT coregistration vs. the drawing of ROIs directly on SPECT images), including ROI size and location. Most authors have used a single ROI for each cerebral lobe. In the present study, several regions within the frontal, temporal, and occipital lobes were independently quantified on the basis of the differences, found on autoradiography, in 5-HT₂ receptor densities in different regions of the same lobe. The differences in ¹²³I-R91150 specific binding among the frontal and occipital subregions, with substantially higher SUR values in the orbitofrontal and calcarine regions, respectively, were consistent with the autoradiography findings

TABLE 3
Reference ^{123}I -R91150 SUR Values Reported in the Literature

| Study | n | Age (y) | Postinjection scanning interval (min) | ^{123}I -R91150 uptake | | | |
|--------------------------|----|---------|---------------------------------------|---------------------------------|-------------|-------------|-------------|
| | | | | Frontal | Temporal | Occipital | Parietal |
| Busatto et al. (17) | 5 | 32.4 | 250 | 1.40 (0.40) | 1.42 (0.42) | 1.42 (0.42) | 1.44 (0.44) |
| Travis et al. (7) | 6 | 29.7 | 120 | 1.33 (0.33) | 1.30 (0.30) | NA | 1.38 (0.38) |
| Baeken et al. (24) | 26 | 26–60 | 120 | 1.78 (0.78) | 1.87 (0.87) | 1.74 (0.74) | 1.71 (0.71) |
| Reneman et al. (20) | 9 | 22.8 | 120 | NA | NA | 1.74 (0.74) | NA |
| Reneman et al. (6) | 10 | 23 | 120 | 0.68* | 0.68* | 0.68* | 0.68* |
| Reneman et al. (5) | 11 | 22.5 | 120 | 1.75 (0.75) | NA | 1.75 (0.75) | 1.85 (0.85) |
| Audenaert et al. (2) | 12 | 29 | 110–140 | 0.68 | NA | NA | NA |
| Audenaert et al. (19) | 11 | 25.6 | 110–140 | 0.94 | 0.91 | 1.03 | 1.02 |
| van Heeringen et al. (1) | 13 | 30.4 | 110–140 | 1.68 (0.68) | NA | NA | NA |
| Versijpt et al. (3) | 26 | 22–85 | 110–140 | 1.66 (0.66) | 1.52 (0.52) | 1.70 (0.70) | 1.65 (0.65) |
| Goethals et al. (23) | 11 | 25.6 | NA | 0.94 | 0.91 | 1.03 | 1.02 |

*Whole cortex.

NA = not available.

Data in parentheses are calculated as $([\text{target-to-cerebellum ratio}] - 1)$ for those studies originally reporting target-to-cerebellum ratios, to allow comparison with SUR values $(\text{target} - \text{cerebellum}/\text{cerebellum})$.

(16). In the only published study with ^{123}I -R91150 in which subregions were independently analyzed, the orbitofrontal region also showed the highest SUR within the frontal lobe (3). The orbitofrontal cortex presents the highest SUR among all cerebral regions and reaches pseudoequilibrium later than do the remaining frontal regions studied. The fact that regions with higher receptor density may reach later equilibrium has been reported (25,26). These particularities of different parts of the same cerebral lobe should be considered in ^{123}I -R91150 quantification.

The potential influence of age, sex, and interhemispheric asymmetry on the final quantification deserves mention. Previous studies of ^{123}I -R91150 in humans showed a decrement of $\pm 1.1\%$ per year (24) and 11.6% per decade (3). The SUR values found in the present study came from 17 subjects in their twenties; therefore, age was not expected to influence the mean SUR values. However, this possibility has to be considered when one is interpreting mean SUR values reported in the literature (Table 3), because some studies have included patients ranging widely in age. Further experience is needed to determine the pseudoequilibrium interval in aged populations, because pseudoequilibrium might be achieved earlier in aged subjects with a low 5-HT_{2A} receptor density than in young subjects. However, given the long pseudoequilibrium interval shown in this study for ^{123}I -R91150, image acquisitions starting at 180–240 min after injection would most likely be within the pseudoequilibrium interval in aged populations as well. Given the reported evidence of lack of differences in ^{123}I -R91150 uptake according to sex, and to avoid radiation exposure in young women, we excluded women from this study (3,24). Finally, because previous studies did not find any significant differences in ^{123}I -R91150 uptake between the left and right hemispheres, averaged values from both hemispheres were used in this study.

The within-scan variability in SUR measurements obtained at different times throughout the pseudoequilibrium interval was acceptable, ranging from 10% to 15%. This variability was in line with the 10%–17% test–retest variability reported using different radioligands for neurotransmission SPECT (26–31). As expected, between-subject variability was higher, ranging from 15% to 35%, therefore suggesting that a within-subject SPECT design be planned whenever possible. The highest within-scan and between-subject variability was found in the superior frontal region, whereas the lowest was in the temporal lobe. These data could be of interest for selecting cortical regions for quantification in particular studies.

Plasma Analysis

No studies of ^{123}I -R91150 stability in plasma or of ^{123}I -R91150 metabolite analysis have been reported. Thus, all samples were processed as soon as possible after blood sampling, and always within 60 min after extraction. Peremans et al. (32) obtained venous blood samples from a dog at different times after ^{123}I -R91150 administration but did not further analyze the samples, calculating only total radioactivity in blood as a function of time. A sharp decrease in radioactivity was found 3 min after injection. At 20 min, a decrease in radioactivity to 2% of the injected dose was noted, and a stable plateau was reached from 20–40 min onward. This finding is consistent with our finding of a sharp decrease in radioactivity after a short time. However, in our case, this decrease occurred 1 min after injection but the plateau occurred 15 min after injection.

Busatto et al. (17) reported total radioactivity in blood over time, relative distribution between plasma and cell compartments, and the protein-bound fraction in plasma in humans. A sharp decrease in radioactivity was noted during the first 20–30 min after injection, after which radioactivity

reached a stable plateau. In the present study, the plateau was reached after 15 min after injection (Figs. 4A and 4B). In addition, Busatto (17) et al. reported that more than 90% of the activity was in the plasma after 30 min after injection, and 62% of the activity bound to proteins after 150 min after injection. Our results showed that the percentage of activity in plasma reached a plateau at 80% (Fig. 6), whereas the fraction of activity linked to protein could not be determined because protein fraction is removed by precipitation of protein with acetonitrile, leading to denaturalization of the protein and thus modifying the binding fraction.

CONCLUSION

^{123}I -R91150 is a useful ligand for SPECT assessment of the 5-HT_{2A} receptor in humans. Cerebral distribution, BP, and SUR₁₈₀ values obtained by this method in healthy volunteers agree with autoradiography results, showing the highest specific binding in cortical regions and low specific binding in subcortical gray matter. BP measured using the full kinetic compartmental model with arterial sampling correlated strongly with BP measured by SRTM and with SUR values measured by TR. These findings suggest that TR can be used for ^{123}I -R91150 SPECT quantification of 5-HT_{2A} receptor binding with a simple protocol avoiding arterial blood sampling and serial scanning over time.

ACKNOWLEDGMENTS

The authors thank Roger N. Gunn, Javier Pavia, Michael Travis, and Emilio Merlo-Pich for meaningful discussions; Eugenio Rabiner, Magi Farre, Fernando Escolano, and Clare Burgess for useful contributions to the design and execution of the protocol; Nuria Merino and Vanessa Gómez for excellent technical assistance; and all the volunteers who participated in the study. This study was supported by the Psychiatry Centre of Excellence for Drug Discovery, Clinical Pharmacology Discovery Medicine/Experimental Medical Sciences, GlaxoSmithKline.

REFERENCES

- van Heeringen C, Audenaert K, Van Laere K, et al. Prefrontal 5-HT_{2A} receptor binding index, hopelessness and personality characteristics in attempted suicide. *J Affect Disord*. 2003;74:149–158.
- Audenaert K, Van Laere K, Dumont F, et al. Decreased frontal serotonin 5-HT_{2A} receptor binding index in deliberate self-harm patients. *Eur J Nucl Med*. 2001;28:175–182.
- Versijpt J, Van Laere KJ, Dumont F, et al. Imaging of the 5-HT_{2A} system: age-, gender-, and Alzheimer's disease-related findings. *Neurobiol Aging*. 2003;24:553–561.
- Goethals I, Vervaeke M, Audenaert K, et al. Comparison of cortical 5-HT_{2A} receptor binding in bulimia nervosa patients and healthy volunteers. *Am J Psychiatry*. 2004;161:1916–1918.
- Reneman L, Enderit E, de Bruin K, et al. The acute and chronic effects of MDMA ("ecstasy") on cortical 5-HT_{2A} receptors in rat and human brain. *Neuropsychopharmacology*. 2002;26:387–396.
- Reneman L, Habraken JB, Majoie CB, Booij J, den Heeten GJ. MDMA ("Ecstasy") and its association with cerebrovascular accidents: preliminary findings. *Am J Neuroradiol*. 2000;21:1001–1007.

- Travis MJ, Busatto GF, Pilowsky LS, et al. 5-HT_{2A} receptor blockade in patients with schizophrenia treated with risperidone or clozapine: a SPET study using the novel 5-HT_{2A} ligand ^{123}I -5-I-R-91150. *Br J Psychiatry*. 1998;173:236–241.
- Jones HM, Travis MJ, Mulligan R, et al. In vivo serotonin 5-HT_{2A} receptor occupancy and quetiapine: an R91150 single photon emission tomography study. *Psychopharmacology (Berl)*. 2001;157:60–66.
- Jones HM, Travis MJ, Mulligan R, et al. In vivo 5-HT_{2A} receptor blockade by quetiapine. *Am J Psychiatry*. 2000;157:148–152.
- Peremans K, Audenaert K, Hoybergs Y, et al. The effect of citalopram hydrobromide on 5-HT_{2A} receptors in the impulsive-aggressive dog, as measured with (123)I-5-I-R91150 SPECT. *Eur J Nucl Med Mol Imaging*. 2005;32:708–716.
- Catafau AM, Danus M, Bullich S, et al. Characterization of the SPECT 5-HT_{2A} receptor ligand ^{123}I -R91150 in healthy volunteers: part II—ketanserin displacement. *J Nucl Med*. 2006;47:929–937.
- Eersels J, Travis MJ, Herscheid J. Manufacturing I-123-labelled radiopharmaceuticals: pitfalls and solutions. *J Labelled Compds Radiopharm*. 2005;48:241–257.
- Bullich S, Ros D, Pavia J, et al. Influence of co-registration algorithms on ^{123}I -IBZM SPET imaging quantification [abstract]. *Eur J Nucl Med Mol Imaging*. 2004;31(suppl):S49.
- Erlandsson K, Bressan RA, Mulligan RS, et al. Kinetic modelling of [^{123}I]CNS 1261: a potential SPET tracer for the NMDA receptor. *Nucl Med Biol*. 2003;30:441–454.
- Lammertsma AA, Hume SP. Simplified reference tissue model for PET receptor studies. *Neuroimage*. 1996;4:153–158.
- Pazos A, Probst A, Palacios JM. Serotonin receptors in the human brain—IV. Autoradiographic mapping of serotonin-2 receptors. *Neuroscience*. 1987;21:123–139.
- Busatto GF, Pilowsky LS, Costa DC, et al. Initial evaluation of ^{123}I -5-I-R91150, a selective 5-HT_{2A} ligand for single-photon emission tomography, in healthy human subjects. *Eur J Nucl Med*. 1997;24:119–124.
- Schotte A, Maloteaux JM, Laduron PM. Characterization and regional distribution of serotonin 5-HT₂-receptors in human brain. *Brain Res*. 1983;276:231–235.
- Audenaert K, Van Laere K, Dumont F, et al. Decreased 5-HT_{2A} receptor binding in patients with anorexia nervosa. *J Nucl Med*. 2003;44:163–169.
- Reneman L, Booij J, Schmand B, van den Brink W, Gunning B. Memory disturbances in "Ecstasy" users are correlated with an altered brain serotonin neurotransmission. *Psychopharmacology (Berl)*. 2000;148:322–324.
- Travis MJ, Visvikis D, Erlandsson K, et al. Displacement of the selective 5-HT_{2A} ligand ^{123}I -5-I-R91150 by unlabelled ketanserin [abstract]. *Schizophr Res*. 2000;41:253.
- Pinborg LH, Adams KH, Svarer C, et al. Quantification of 5-HT_{2A} receptors in the human brain using [^{18}F]altanserin-PET and the bolus/infusion approach. *J Cereb Blood Flow Metab*. 2003;23:985–996.
- Goethals I, Vervaeke M, Audenaert K, et al. Comparison of cortical 5-HT_{2A} receptor binding in bulimia nervosa patients and healthy volunteers. *Am J Psychiatry*. 2004;161:1916–1918.
- Baeken C, D'haenen H, Flamen P, et al. ^{123}I -5-I-R91150, a new single-photon emission tomography ligand for 5-HT_{2A} receptors: influence of age and gender in healthy subjects. *Eur J Nucl Med*. 1998;25:1617–1622.
- Olsson H, Halldin C, Swann CG, Farde L. Quantification of [^{11}C]FLB 457 binding to extrastriatal dopamine receptors in the human brain. *J Cereb Blood Flow Metab*. 1999;19:1164–1173.
- Catafau AM, Pérez V, Penengo MM, et al. SPECT of serotonin transporters using ^{123}I -ADAM: optimal imaging time after bolus injection and long-term test-retest in healthy volunteers. *J Nucl Med*. 2005;46:1301–1309.
- Abi-Dargham A, Zea-Ponce Y, Terriere D, et al. Preclinical evaluation of [^{123}I]R93274 as a SPECT radiotracer for imaging 5-HT_{2A} receptors. *Eur J Pharmacol*. 1997;321:285–293.
- Varrone A, Fujita M, Verhoeff NP, et al. Test-retest reproducibility of extrastriatal dopamine D₂ receptor imaging with [^{123}I]epidepride SPECT in humans. *J Nucl Med*. 2000;41:1343–1351.
- Tsuchida T, Ballinger JR, Vines D, et al. Reproducibility of dopamine transporter density measured with ^{123}I -FPCIT SPECT in normal control and Parkinson's disease patients. *Ann Nucl Med*. 2004;18:609–616.
- Seibyl JP, Laruelle M, van Dyck CH, et al. Reproducibility of iodine-123-beta-CIT SPECT brain measurement of dopamine transporters. *J Nucl Med*. 1996;37:222–228.
- Catafau AM, Bullich S, Penengo M, et al. Test-retest reliability of ^{123}I -IBZM SPECT measurement of free striatal dopamine D₂ receptors in healthy volunteers [abstract]. *Eur J Nucl Med Mol Imaging*. 2005;32(suppl 1):S82.
- Peremans K, Audenaert K, Jacobs F, et al. Biodistribution and displacement studies of the selective 5-HT_{2A} receptor antagonist ^{123}I -5-I-R91150 in the normal dog. *Nucl Med Commun*. 2002;23:1019–1027.